# Extended Ellipse Model for Multi-Polarized MIMO Antennas

Sewoong Kwon[1], Hyun-Wook Moon[1], Jae-Woo Lim[2], Cheol Mun[3], Young Joong Yoon[1]
[1] *Center for Information Technology Microwave and antenna lab., Department of Electrical and Electronics Engineering, Yonsei University*
[2] *Ministry of Information and Communication Radio Research Laboratory*
[3] *Department of Electronic Communication Engineering, Chungju National University*
*E-mail : iceberg@ yonsei.ac.kr*

**Abstract**

*This work presents a quasi-three dimensional scattering model to predict the polarization properties of an indoor radio channel. The proposed model considers not only the effect of the polarization of fields scattered by scatterers but also extends the ellipse model to a quasi-three dimensional model. In the model, all scatterers are considered as a patch scatterer and distribution properties of the angle and delay correspond with those of an ellipse model. Vertical and horizontal ellipse planes are employed to consider the floor, ceiling, walls, and extraneous structures. For a realistic indoor channel model, multi ellipses are defined so as to incorporate indoor channel properties. Investigation of the polarization matrix of the model is conducted in terms of cross-polarization discrimination (XPD) and MIMO capacity by the Monte-Carlo method. The results demonstrate that the model can predict various properties for multi-polarized antennas.*

## 1. INTRODUCTION

POLARIZATION diversity plays an important role not only in traditional wireless communication but also in recent multi-antenna wireless communication such as Multiple Input Multiple Output (MIMO). The simplest model for considering polarization is the cross polarization discrimination (XPD) based polarization model. In this model, polarization properties are defined in a simple matrix form of XPD levels and the polarized channel can be generated by multiplying it to a result channel impulse response [1]. While this model is simple the channel variety is low and the process of obtaining the XPD level is frequently obtained by measurement. Because the XPD levels have insufficient environment generality, this model cannot be used as a generalized channel model. Recently, a stochastic geometry-based scattering model extended to multi-polarized transmissions was proposed for an outdoor LOS environment [2]. This model has a multi-tier ellipse geometry and each scattering process is statistically described by a matrix reflection coefficient corresponding to dual-polarization states. The model also allows for simulation of the effects of the range on the K-factor, delay-spread, Doppler spectrum, channel correlations and capacity, branch power ratio, and cross-polar discrimination. However, while it can consider 2D or 3D scatterer distributions, 2D scatterer distribution because transceiver station (BTS) antennas in BWA systems have relatively narrow beamwidth in the vertical direction. Moreover, because the model is suitable for microcell or macrocell scenarios, some suppositions such as a 2D scatterer or a circular scatterer free zone are not appropriate for an indoor channel model. It was reported that a three-dimension extension of the 3GPP spatial channel model could effect the correlation of a channel [3].

In the present work, the indoor multi-polarized channel property is modeled with dually polarized antenna elements. To this end, an ellipse model is selected, as this model has many properties for indoor channels[3]. Furthermore, properties for indoor picocell LOS scenarios are considered. To do so, the electromagnetic polarization properties of the scatterers are defined and a three-dimensional extension is considered: as a three-dimensional model is required for an indoor channel due to the presence of a floor, low ceiling, and arbitrary appliances. Finally, we extend the model such that it can address the polarization angle of MIMO antennas for an indoor picocell indoor LOS channel.

## 2. MULTI-POLARIZED INDOOR CHANNEL MODEL

### *A. Multi-tier ellipse model*

As the distance and height difference between the transmitting antenna and the receiving antenna are respectively small and scatterers are distributed around the transmitter and the receiver in an indoor environment, an ellipse model such as the GBSB (Geometrically Based Single Bounce) model is suitable for representing the channel properties in a LOS indoor environment [4]. The multi-tier ellipse model is shown in Figure 1. Scatterers are taken as being uniformly distributed on the region bounded by an n ellipse defined by the parameters $(a,b,f)$ . The notations '$a$' and '$b$' are the major and minor axes of an ellipse, respectively, and the '$f$' is the distance between the focus of the ellipse and the origin. It is considered that the transmitter at the left foci transmits to the mobile at the right foci. In an ellipse model, the delay of

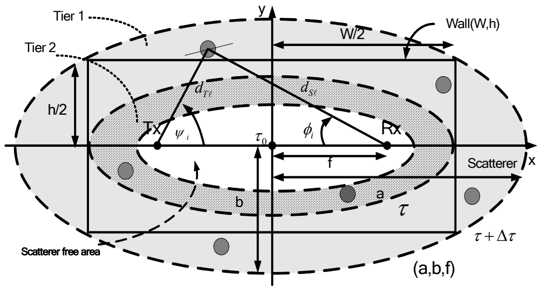


Figure 1. Basic ellipse model bounded by an ellipse with transmitter and receiver at the foci

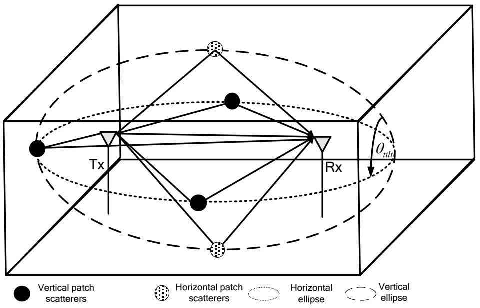


Figure 2. Quasi-three dimensional ellipse model for an indoor multipath channel

the channel impulse response has a value between $\tau$ and $\tau+\Delta\tau$ . Scatterers are classified by their time delay properties and a scatterer free area is defined to preserve the LOS condition. Hence, the scatterer free area ellipse definition follows the definition of a First Fresnel zone. It is considered reasonable that the LOS condition is defined by a Fresnel zone in a small area [5].

The notation 'h' and 'W' are the height and width of a rectangular wall, respectively. For these suppositions, the delay $\tau_0$ of a direct wave, minimum delay $\tau_{\min}$ of an ellipse of a first Fresnel zone, and maximum excess delay $\tau_{\max}=\tau+\Delta\tau$ are defined respectively.

$$\tau_0 = 2f/c \tag{1}$$

$$\tau_{\min} = \frac{2}{c}\sqrt{\frac{c}{4f}+f^2} \tag{2}$$

$$\begin{aligned}\tau_{\max} &= 2a/c \\ &= \frac{1}{c}\left(\begin{array}{l}\sqrt{(W/2+f)^2+(h/2)^2} \\ +\sqrt{(W/2-f)^2+(h/2)^2}\end{array}\right)\end{aligned} \tag{3}$$

As a normal to a tangent line to an ellipse equally divides the angle that is made by a segment of a line from a left foci to a point of contact and a segment of a line from a right foci to a point of contact, the incident angle $\theta_i$ at the scatterer can calculated by $\psi_\ell$ and $\phi_\ell$ .

$$\theta_i = \frac{|\psi_\ell - \phi_\ell|}{2} \tag{4}$$

$d_{T\ell}$ is the distance between the transmitting antenna and the center of the ℓ'th scatterer. $d_{R\ell}$ is the distance between the receiving antenna and the center of the ℓ'th scatterer. The second law of cosine is used to obtain the distance $d_{T\ell}$ .

$$d_{T\ell} = \frac{a_\ell^2 - f^2}{a_\ell - f\cos(\psi_\ell)} \tag{5}$$

$$d_{R\ell} = 2a_\ell - d_{T\ell} \tag{6}$$

$\psi_\ell$ and $\phi_\ell$ are generated with a cumulative density function and a uniform random variable and $a_\ell$ is the length of the major axis of an ellipse containing the $\ell$ 'th scatterer. The process for generating the angle and delay of the ellipse model follows that described by Liberti et al [4].

*B. Scattering waves with arbitrary polarization*

The relation between the incidence wave and the scattered wave is determined by the polarization scattering matrix **S** with the element $\mathbf{s_{11}}$.

$$\begin{bmatrix}\vec{\mathbf{e}}_\perp^s(\boldsymbol{\theta}_\mathbf{s}) \\ \vec{\mathbf{e}}_{II}^s(\boldsymbol{\theta}_\mathbf{s})\end{bmatrix}_\ell = \begin{bmatrix}\mathbf{s}_{11}(\boldsymbol{\theta}_\mathbf{i},\boldsymbol{\theta}_\mathbf{s}) & \mathbf{s}_{12}(\boldsymbol{\theta}_\mathbf{i},\boldsymbol{\theta}_\mathbf{s}) \\ \mathbf{s}_{21}(\boldsymbol{\theta}_\mathbf{i},\boldsymbol{\theta}_\mathbf{s}) & \mathbf{s}_{22}(\boldsymbol{\theta}_\mathbf{i},\boldsymbol{\theta}_\mathbf{s})\end{bmatrix}_\ell \begin{bmatrix}\vec{\mathbf{e}}_\perp^{\,i}(\boldsymbol{\theta}_\mathbf{i}) \\ \vec{\mathbf{e}}_{II}^{\,i}(\boldsymbol{\theta}_\mathbf{i})\end{bmatrix}_\ell \tag{7}$$

where ℓ is the index of a scattering patch among many scattering patches. $\boldsymbol{\theta}_S$ and $\boldsymbol{\theta}_i$ are the angle vectors $[\theta_S,\phi_S]$ and $[\theta_i,\phi_i]$ , respectively. $\theta_i$ , $\phi_i$ , $\theta_s$ , $\phi_s$ are the angle of incidence, the angle of scattering in the elevation direction, and the angle of scattering in the azimuth direction, respectively.

When the scatterer is diffracted, the scattering matrix **S** should be filled with diffraction coefficients while for the reflection case it should be filled with reflection coefficients.

The reflection is applicable to smooth surfaces only. When the surface is made progressively rougher, the incident wave is scattered [6]. The degree of scattering depends on the angel of incidence and the roughness of the surface in comparison to the wavelength. A patch scattering model has been proposed to predict the path loss of a microcellular radio channel in an urban environment [7]. Hence, we apply the model to the picocell model in an indoor environment.

Incident fields for considering polarization are

$$\vec{\mathbf{e}}^{i}_{\perp,\ell}(\boldsymbol{\theta}_{\mathbf{i}}) = \vec{\mathbf{e}}^{i}_{\ell}\cos\theta^{i}_{p} \tag{8}$$

$$\vec{\mathbf{e}}^{i}_{II,\ell}(\boldsymbol{\theta}_{i}) = \vec{\mathbf{e}}^{i}_{\ell}\sin\theta^{i}_{p} \tag{9}$$

*C. Extended multi-polarized ellipse model*

The polarization of a wave can be changed by the relationship between the normal vector direction of a diffracting or scattering surface and the polarization of the incidence wave. The indoor environment is characterized by a number of horizontal planes and vertical planes of the indoor space and fixtures, as well as the polarization property, which is influenced by the indoor propagation environment. For this reason the 2-D ellipse model must extended to 3-D ellipse model. For simplicity, we use only two ellipses for the three-dimensional ellipse model instead of a three dimensions ellipsoid model. There are reflection planes that are perpendicular to each other in the indoor space, and these planes can be classified as a horizontal plane, such as the floor and ceiling, and a vertical plane, such as walls. Moreover, because the shapes of fixtures in the indoor space can generally be simplified as rectangular parallelepiped objects, fixtures have horizontal and vertical planes. Two ellipses are defined with the tilt angle of the ellipse, $\theta^{tilt}$ . It is assumed that patches are placed with a uniform distribution on an ellipse and the normal vector of a patch is normal to the ellipse. Hence, $\vec{\theta}_i$ is irrespective of the ellipse tilt angle, $\theta_{tilt}$, and $\vec{\theta}_s$ is equal to $\vec{\theta}_i$ because of the property of the ellipse.

$$\boldsymbol{\theta}_i = [\theta_i, \phi_{patch}] \tag{10}$$

$$\boldsymbol{\theta}_S = [\theta_i, \pi - \phi_{patch}] \tag{11}$$

The notation '$\phi_{patch}$' is the azimuth angle of the patch to the incident angle. For example, the angle $\phi_{patch}$ is an angle of $\hat{u} - \hat{x}$ in the case of a V-plane ellipse. In this paper, $\phi_{patch}$ is considered as a uniform distribution $U[0,\pi)$ . The accuracy of the polarization coupling mechanism is very important with respect to the prediction of channel polarization properties. A reflection cannot change a vertical polarization to a horizontal polarization or vice versa. Hence, the coupling mechanism is diffraction and scattering. In this model, the polarization coupling caused by scattering is considered. In this mode, polarization coupling is caused by the azimuth angle of a patch.

The other important angles are the polarization angles, $\theta^i_p$ and $\theta^s_p$ . The vertical and horizontal ellipse planes have $\theta^{tilt} = 0^\circ$ and $\theta^{tilt} = 90^\circ$, respectively. If a transmit antenna is a vertically polarized Herzian dipole, its tilt angle $\theta_{TX}$ is $0^\circ$ and polarization angle $\theta^i_p$ is

$$\theta^i_p = \theta^{tilt} - \theta_{TX} \tag{12}$$

The polarization angle of the scattered wave $\theta^s_p$ is given as

$$\theta^s_p = \tan^{-1}\left(\frac{\mathbf{e}^S_{II}}{\mathbf{e}^S_{\perp}}\right) \tag{13}$$

For the receiver case, its tilt angle $\theta_{RX}$ is $0^\circ$ and the polarization angle $\theta^r_p$ is

$$\theta^r_p = \theta^{tilt} - \theta_{RX} \tag{14}$$

The received field $\mathbf{e_r}$ is

$$\mathbf{e}_{r,l} = \mathbf{e}_{\perp,l}\cos(\theta^r_p - \theta^S_{p,l}) + \mathbf{e}_{II,l}\sin(\theta^r_p - \theta^S_{p,l}) \tag{15}$$

*D. MIMO extension of the extended ellipse model*

The extended multi-polarized ellipse model is used for the element of a MIMO channel matrix H. The received signal $\mathbf{y}$ at the receiving antennas can be expressed as

$$\mathbf{y} = \mathbf{Hx} + \mathbf{n} \tag{16}$$

The matrix **H** is a channel matrix that is composed of steering matrices and Single Input and Single Output channel impulse responses. Hence, the received signal at the $l$'th snapshot can be expressed as

$$\mathbf{y}_l = (\vec{\mathbf{s}}_l(\mathbf{a_R}\mathbf{a_T^T}))\mathbf{x}_l + \mathbf{n} \tag{17}$$

$\mathbf{a_T}$ and $\mathbf{a_R}$ are the angle steering vectors of the transmitter side and receiver side, respectively. A steering vector is expressed as

$$\mathbf{a}(\theta,\phi) = [1\ e^{j(u+v+w)}\ \cdots\ e^{j((n_x-1)u+(n_y-1)v+(n_z-1)w)}] \tag{18}$$

where $u = \frac{2\pi d_x}{\lambda}\cos\phi\cos\theta, v = \frac{2\pi d_y}{\lambda}\cos\phi\sin\theta, w = \frac{2\pi d_z}{\lambda}\sin\phi$

When the transmit signal vector $\mathbf{x}$ is an impulse, the vector $\mathbf{s}_l$ is defined as a field component of the $l$'th impulse response at a Single Input Single Output channel.

*E. Parameter definitions*

For a narrowband channel, when channel state information is unknown, its channel power is uniformly allocated. Hence, the channel capacity is defined as [1]

$$C(l) = \sum_{i=1}^{min(M_T, M_R)} log_2\left(1 + \frac{E_s}{M_T N_0}\lambda_i(l)\right) \quad (19)$$

$E_S/N_0$ is the signal to noise ratio and $\lambda_i(l)$ is an eigenvalue of $\mathbf{H}(l)\mathbf{H}(l)^H$.

The ergodic capacity is defined as

$$C = E\{C(l)\} = \frac{1}{L}\sum_{l=1}^{L} C(l) \quad (20)$$

### 3. Results of the Proposed Model

In order to verify the proposed model, the basic parameters listed in Table 1 (the parameters of a small office room [8]) are applied to the model.

In an indoor LOS single bounce scenario, the largest time delay is caused by walls, floor, and ceiling. Hence, the scatterers of the outer ellipse area are composed of a reflecting scatterer. Scatters of an inner ellipse area are composed of a scattering scatterer. Figure 3 shows the simulated antenna configurations. Figure 3(a) is two vertical MIMO antennas spaced at 0.5 λ. Figures 3(b) and Figure 3(c) each display a MIMO antenna configuration spaced at 0.5 λ. Figure 3(d) is a polarized MIMO antenna with 90° polarized antennas.

The simulated results are shown from Figure 4 to Figure 6. The mean Ricean K factor level of the model is 4 dB. The Ricean K factor level for an indoor LOS scenario is known to be 4 dB for the scatterer LOS path [9]. The channel capacity for a 2 by 2 MIMO antenna in this environment is shown in Figure 5 and Figure 6. For this environment, the 'VH' and 'P90' antenna configuration, respectively, have more gain because of their polarization channel effect. Moreover, when there is an LOS direct wave, the polarized antenna has more capacity than the uni-polar antenna configuration.

Their outage properties with a direct wave are better than that of the case without a direct wave.

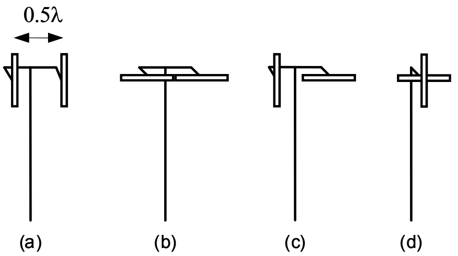


Figure 3. Antenna configurations
(a) Two verticals (VV) (b) Two horizontals (HH) (c) Vertical-horizontal (VH)
(d) 90° polarized (P90)

TABLE 1 Basic parameters for simulation

| parameter | Description | value |
|---|---|---|
| W | Width for h plane | 8.09 m |
| $H_v$ | Height for v plane | 3.6 m |
| $H_h$ | Height for h plane | 5.37 m |
| f | distance from the origin to a focus | 2.5 m |
| $NT_h$ | The number of tiers for h plane | 2 |
| $NT_v$ | The number of tiers for v plane | 2 |
| $n_t$ | The number of transmitting antennas | 2 |
| $n_r$ | The number of receiving antennas | 2 |
| Freq | RF frequency | 2.375 GHz |

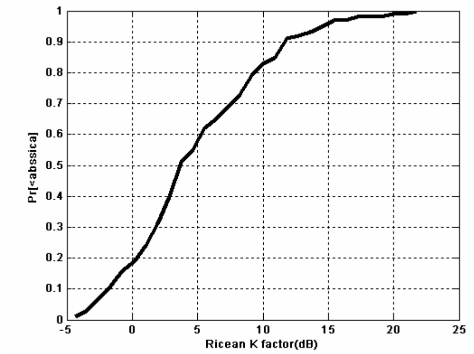


Figure 4. Ricean K factor CDF of the proposed model

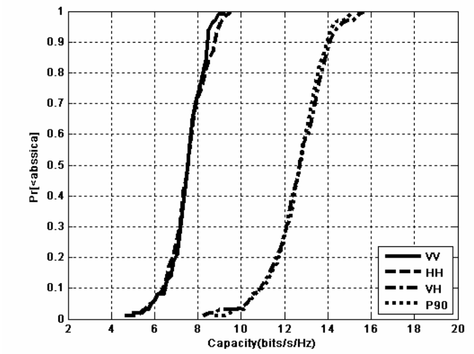


Figure 5. Channel capacity with a direct wave

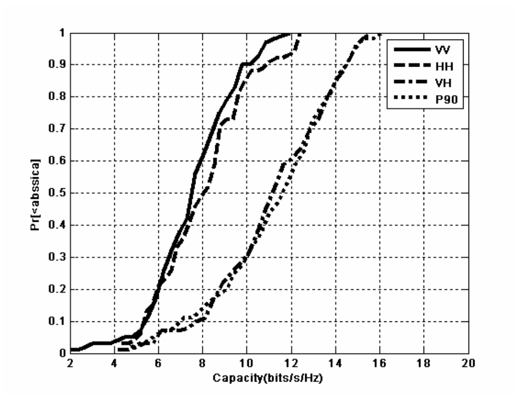


Figure 6. Channel capacity without a direct wave

## 4. CONCLUSIONS

This work presents an indoor polarized channel model that is capable of considering 3-D scattering and polarization for an indoor environment. Moreover, the model has more parameters for indoor scenarios and it can deal multi-polarized MIMO antenna configuration as well as multi-polarized Single Input and Single Output (SISO) channel properties. The results demonstrate that the model can predict a multi-polarized MIMO channel for an indoor environment because it models the indoor polarized propagation mechanism and has been extended for a MIMO antenna. In future study, the model will be extended for various indoor environments.

## REFERENCES


[1] A. J. Paulraj et al, *Introduction to Space-Time Wireless Communications*(Cambridge, 2003)

[2] C. Oestges, V. Erceg, and A. J. Paulraj, Propagation Modeling of MIMO Multipolarized Fixed Wireless Channel, *IEEE Transaction on Vehicular Technology, 53(3)*, pp. 644-654, May 2004.

[3] L. Krasny, Karl J. Molnar, Radio Channel Models for MIMO Antenna Systems Based On Ellipsoidal Scattering, *Global Telecommunication Conference 2004(6)*, Nov.29~Dec.3, pp. 3969-3973, 2004

[4] J. C. Liberti, T. S. Rappaport, A geometrically based model for line-of-sight multipath radio channels, *IEEE Vehicular Technology Conference, 'Mobile Technology for the Human Race'., 46th(2)*, pp. 844-848, April 1996.

[5] H. L. Bertoni, *Radio Propagation for Model Wireless Systems* (Upper Saddle River, NJ: Prentice-Hall, 2000).

[6] C. A. Balanis, *Advanced Engineering Electromagnetics* (John Wiley & Sons Inc., 1989)

[7] J. H. Tarng, K. M. Ju, A Novel 3-D Scattering Model of 1.8-GHz Radio Propagation in Microcellular Urban Environment, *IEEE Transaction on Electromagnetic Compatibility(41)*, no. 2, pp. 100-106, 1999.

[8] S. Kwon, S. Ryu, B. Lee, J. Seok, C. Mun, Y. J. Yoon, A Study on Spatial characteristics of an indoor multi-antenna channel, *International Symposium on Antennas and Propagation 2005(1)*, pp. 55~58, 3-5, Aug, 2005.

[9] A.K. Jagannatham, V.O Erceg., MIMO indoor WLAN channel measurements and parameter modeling a 5.25 GHz, *IEEE 60th Vehicular Technology Conference, 2004. VTC2004-Fall (1)*, pp. 106 - 110 26-29 Sept. 2004